Interactions between Surfaces Bearing End-Adsorbed Chains in a Good Solvent

Hillary J. Taunton,[†] Chris Toprakcioglu,[†,‡] Lewis J. Fetters,[§] and Jacob Klein*[,∥]

Cavendish Laboratory, Madingley Road, Cambridge CB3 0HE, England, Institute of Food Research, AFRC, Colney Lane, Norwich NR4 7UA, England, Exxon Research and Engineering Corporation, Annandale, New Jersey 08801, and Polymer Research, Weizmann Institute of Science, Rehovot 76100, Israel. *Received April 3, 1989; Revised Manuscript Received June 26, 1989*

ABSTRACT: We have measured the force–distance profiles between two curved mica sheets immersed in toluene and in xylene, both in the pure solvents and following addition of polystyrene (PS), end-functionalized polystyrene of different molecular weights M, PS–X(M), and polystyrene–poly(ethylene oxide) diblock copolymers (PS–PEO) with a short PEO block. Our results show that PS does not adsorb from the (good solvents) toluene and xylene but that once PS–X or PS–PEO are added to the solution the surface is rapidly covered, showing that the nonadsorbing PS tails are anchored at one end only. The force profiles following surface coverage are monotonically repulsive, and the range $2L_0$ for onset of interaction is roughly twice that of the corresponding adsorbed chains. There is no evidence of bridging attraction at low surface coverage or of finite relaxation times following strong compression, both of which are characteristic of adsorbed chains. The qualitative behavior with both PS–X and PS–PEO is very similar. For the PS–X(M), we find $L_0 \propto M^{0.6}$, and we are also able to estimate the mean interanchor spacing s and find it to increase markedly with M. These features are in accord with equilibrium expectations for a fixed anchoring energy of the polystyrene on the mica. We find that our data are well fitted quantitatively both by scaling and by mean-field models.

I. Introduction

Two solid surfaces bearing a high surface coverage of adsorbed flexible polymer repel each other strongly as they approach in a good-solvent medium, and this despite the mutual van der Waals attractions between the underlying surfaces themselves. This effect is due to the large osmotic repulsions between segments in the opposing layers, and its use in the steric stabilization of colloidal dispersions is well established.[1,2] In recent years the forces between two smooth surfaces bearing adsorbed flexible chains have been extensively studied and have provided insights into the nature of polymer-modified surface interactions.[3] In particular, the attractive *bridging* effect due to polymer chains simultaneously adsorbed on both surfaces was shown to play an important role, especially at low surface coverage by the polymer,[4] and even in good-solvent conditions.[5] Since the route to the (repulsive) high surface coverage regime generally proceeds through a stage of low surface coverage by the adsorbed chains (with bridging-attraction dominance), problems of flocculation in colloidal dispersions can occur on the way to the desired sterically stabilized system.[2,6] This is frequently overcome by using grafted or end-adsorbed chains as steric stabilizers:[7] in this situation one end only of the chain is attached to the surface (either physisorbed or chemically bonded), while the rest of the chain contour is nonadsorbing (and hence nonbridging) and dangles out into solution. Diblock copolymers, with one of the blocks adsorbing and the other nonadsorbing, can lead to similar configurations, though the adsorbing block should be sufficiently short to ensure absence of bridging.

Earlier direct studies of forces between solid surfaces bearing polymeric or oligomeric surfactants, which have been interpreted in terms of an adsorbing moiety and nonadsorbing tail, have been reported in a number of cases: these include anionic alkyl–poly(ethoxy) surfactants in aqueous media,[8,9] where the anchoring moiety is an oligomeric alkyl section and the nonadsorbing tail is the poly(ethoxy) chain. The nonadsorbance of the homopolymer polystyrene (PS) onto mica from toluene, observed earlier,[10] makes this polymer a convenient choice as a nonadsorbing tail in the surface force studies; this has led to measurements between mica surfaces immersed in toluene solutions of diblock copolymers where one of the components is polystyrene or a related polymer. The force measurements in solutions of poly(vinylpyridine)–polystyrene (PVP–PS) by Hadziioannou et al.[11] and PVP–poly(*tert*-butylstyrene) by Ansarifar and Luckham,[12] where in both cases the PVP block is assumed to adsorb while the styrene block is assumed nonadsorbing, fall into this category. All these studies show broadly monotonic repulsion as the surfaces approach each other; the use of PVP anchoring blocks that are comparable in size to the nonabsorbing block, and that are intrinsically insoluble, may in addition lead to interesting surface structures[13] and to behavior that combines characteristics both of adsorbing and nonadsorbing chains.[34]

In the present experiments we sought a system that would mimic a layer of end-grafted polymer chains as closely as possible. To this end, we used nonadsorbing chains (polystyrene in toluene and xylene, both good solvents, with mica as a substrate) with a single polar functional group at one end of the polymer: after some trials a functional group was found that would anchor the chains to the mica. (Polystyrene chains having $-N(CH_3)_2$ and $-COOH$ terminal groups failed to adsorb onto the mica in these conditions.) A similar effect was achieved by bonding a short poly(ethylene oxide) (PEO) moiety onto the PS chains: PEO is known to adsorb onto mica from toluene.[15]

In this paper we describe a comprehensive study of interactions between two surfaces bearing polystyrene

[†] Cavendish Laboratory.
[‡] Institute of Food Research.
[§] Exxon Research and Engineering Corporation.
[∥] Weizmann Institute of Science. Incumbent of Herman Mark Chair in Polymer Physics.

0024-9297/90/2223-0571$02.50/0

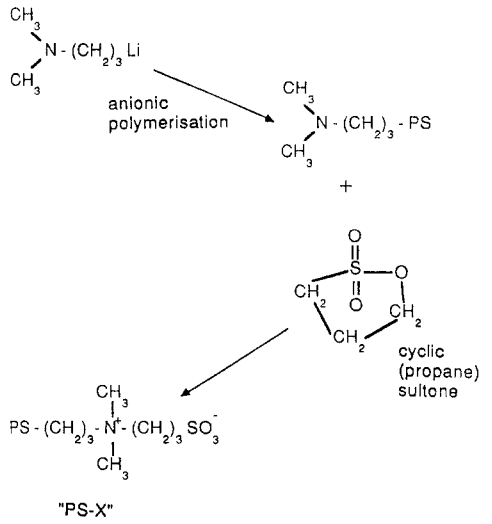

Figure 1. Schematic synthesis route of PS–X.

Table I
Molecular Characteristics of PS–X

sample	M_w[a]	M_w/M_n	R_o,[b] Å	R_F,[b] Å
PS–X(26K)	26 500	1.02	112	122
PS–X(58K)	58 000	1.10	169	197
PS–X(140K)	140 000	1.03	258	323
PS–X(375K)	375 000	1.03	422	575
PS–X(660K)	660 000	1.02	559	801

[a] The molecular weights were determined by size-exclusion chromatography. [b] Both the unperturbed end-to-end dimension R_o and the swollen (Flory) end-to-end dimension R_F refer to the PS chain.[40]

chains anchored to each surface by a single group at one end only, immersed in a good-solvent medium.[16] The case of diblock PS–PEO copolymers with a short adsorbing (PEO) block and a long nonadsorbing (PS) block is also considered. In sections II and III we describe the experimental procedure and data; the results are discussed in the final section, with particular reference both to scaling models and recent mean-field treatments of such interactions.

II. Experimental Section

(a) Materials. Two different methods of anchoring nonadsorbing polystyrene chains to the mica surfaces were employed as noted above. In the first case linear polystyrenes with one end terminated by the zwitterionic group $-(CH_2)_3N^+(CH_3)_2-(CH_2)_3SO_3^-$ were synthesized using the route shown in Figure 1. The molecular characteristics of these polymers, determined by size-exclusion chromatography, are given in Table I. We refer to these end-functional chains as PS–X (or PS–X(M) when specifying a chain of molecular weight M). As was the case for zwitterion-terminated polyisoprenes,[17] [(dimethylamino)propyl]lithium was the initiator. Polymerization was conducted at 30 °C in a benzene–cyclohexane mixture, with the exception of sample PS–X(58K), which was polymerized in cyclohexane at 37 °C. The absence of benzene led to an obviously slower rate of initiation, which is reflected in the M_w/M_n ratio for this sample.

The second group consists of polystyrene–poly(ethylene oxide) diblock copolymers, PS–PEO (or PS–PEO(M)), purchased from Polymer Laboratories (U.K.), who also supplied the molecular characteristics (Table II).

Finally, unfunctionalized linear polystyrene (designated simply PS) was used as a control. This was anionically synthesized and terminated by *sec*-butyl and phenyl groups at its respective ends. Its molecular characteristics are

$$M_w = 1.31 \times 10^5 \qquad M_z/M_w = M_w/M_n = 1.03$$

Solvents employed, BDH Analar or Aristar grade toluene and xylene, were used as received and generally introduced into the apparatus through 0.22-μm prewashed Fluoropore filters. All cleaning solvents were of Analar quality and the water used for rinsing was triply distilled.

(b) Experimental Method. We used the mica force-balance technique, which has been described in detail previously;[18–20] both the apparatus at the Weizmann Institute and that at the Cavendish were utilized; results for similar experiments were identical (within scatter) in both laboratories.

The experiment allows the force $F(D)$ between two curved mica surfaces (mean radius of curvature $R \cong 1$ cm) to be measured as a function of their separation D in the range 0–3000 Å. Separations are determined by white light interferometry to an accuracy of about 3 Å. The optical technique also allows the refractive index of the medium separating the mica surfaces to be determined and hence an estimate of the amount of adsorbed species to be made.[20,21]

At the commencement of each experiment the clean mica surfaces were brought into contact in air as a check that no contamination was present and in order to give a zero surface separation point relative to which all subsequent separations could be calculated. The surfaces were then separated, and the pure solvent, toluene or xylene, was introduced into the apparatus. The forces between the surfaces in the absence of any polymer were then measured.

The unfunctionalized polystyrene was at that stage added to the solvent to a concentration 10^{-6}–10^{-7} mol/L ($\sim 10^{-4}$–10^{-5} w/w), and the force profiles were measured again after a 12-h incubation in the PS solution. Finally, PS–X or PS–PEO was added to the solution, to concentrations 10^{-4}–10^{-5} w/w, and the surface interaction profiles were measured again at different times following introduction of the polymer.

III. Results

(a) Pure Solvent. The interaction between the mica surfaces in the pure toluene or xylene medium was very similar to force profiles in undried organic solvents reported earlier.[10] Typical results are shown in Figure 2: little interaction down to a separation $D \sim 150$ Å, following which a short-range attraction causes a jump of the surfaces into contact. Identical behavior was observed both in toluene and in xylene. Indeed, we found that, within the scatter, results of all measurements in this study were identical in both solvents, and we shall henceforth relate to one or the other interchangeably. While the short-range attraction (Figure 2) resembles a van der Waals interaction between the bare mica sheets, it is probably due, in part, to capillary attraction arising from water condensation into a microdroplet between the surfaces.[22]

(b) Addition of Unfunctionalized PS. When the pure solvent was replaced by a solution of the unfunctionalized polystyrene of concentration 10^{-6} mol/L ($\sim 10^{-4}$ w/w), no measurable difference in the interaction profile was observed even after 12 h of incubation (see Figure 2). Thus we conclude that unfunctionalized PS does not adsorb onto mica from undried toluene or xylene. This is in agreement with the earlier observations of Luckham and Klein.[10] Depletion forces (if present) are too small to be resolved by the apparatus at these concentrations. This stage of the experiment is an essential control to ensure that in the conditions used no polystyrene adsorbs onto the mica surfaces. Once this point was established, however, many of the subsequent profiles were determined without the preaddition of the unfunctionalized PS: results (within scatter) were the same with or without this addition.

(c) Addition of PS–X or PS–PEO. On addition of a solution of PS–X or PS–PEO to a concentration 10^{-6}–10^{-7} mol/L ($\sim 10^{-4}$ w/w), a change in the force profiles was found within about 30 min of adding the new solution, with the attraction being replaced by a strong repul-

Table II
Molecular Characteristics of PS–PEO Obtained from and Characterized by Polymer Laboratories (U.K.)

sample	M_w	M_w/M_n	PEO content,[a] %	$(PS)_x(PEO)_y$ wt av dp x	y	R_F,[b] Å
PS–PEO(150K)[c]	150 000	1.16	1.5	1420	51	340
PS–PEO(184K)[d]	184 000	1.10	4	1700	167	393

[a] Determined by NMR. [b] R_F refers to the Flory end-to-end dimension of the PS block. The values given have a small correction for the sample polydispersities. [c] A minor amount of PS–PEO–PS diblock was indicated for this sample by the SEC traces. [d] The values of the PEO content and the weight-averaged dp values x and y for this sample given in Table I of ref 14 are in slight error.

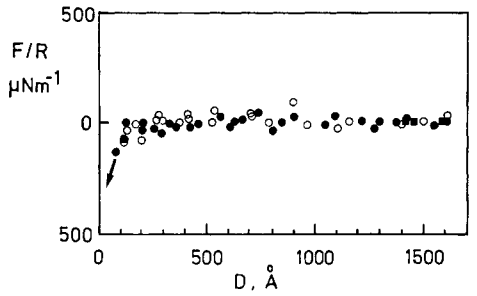

Figure 2. Interaction between curved mica sheets in polymer-free xylene (○) and in the same solvent following addition of unfunctionalized polystyrene and a 12-h incubation (●). Results with toluene were identical within the scatter. The arrow indicates a jump into contact.

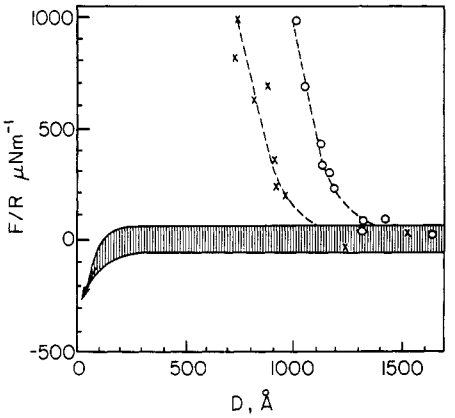

Figure 3. Force–distance profile between two curved mica surfaces (radius R) immersed in a solution (ca. 10^{-4} w/w) of PS–PEO(150K) in toluene and held at a surface separation of ca. 40 μm. The crosses are for a profile measured after 30 min of incubation, while the circles show the force measured 12 h later (equilibrium coverage). The shaded band covers the scatter of the force profile in polymer-free solvent, taken from data as in Figure 2.

sion, as shown in Figure 3 for PS–PEO(150K). Having already established that PS does not adsorb onto mica under the conditions of the experiment (Figure 2), we conclude that the chains have become terminally attached to the surfaces via the zwitterionic group, "X", or the short length of PEO, respectively.[35]

The time for saturation surface coverage to be attained, determined by the point at which no further change was found in the force profile, was variable, being affected by the surface separation, room temperature, and amount of stirring. In general, the adsorption was found to be extremely rapid both for the amphiphilic PS–X and for the PS–PEO diblock copolymer. Even when attempts were made to diffusion limit the adsorption process by keeping the surfaces only 40 μm apart, large repulsions were already found after 30 min of incubation (Figure 3). In most experiments saturation coverage was achieved within 2–3 h. This is appreciably more rapid than the rates of adsorption that have typically been found for adsorbing homopolymers in similar conditions, where the

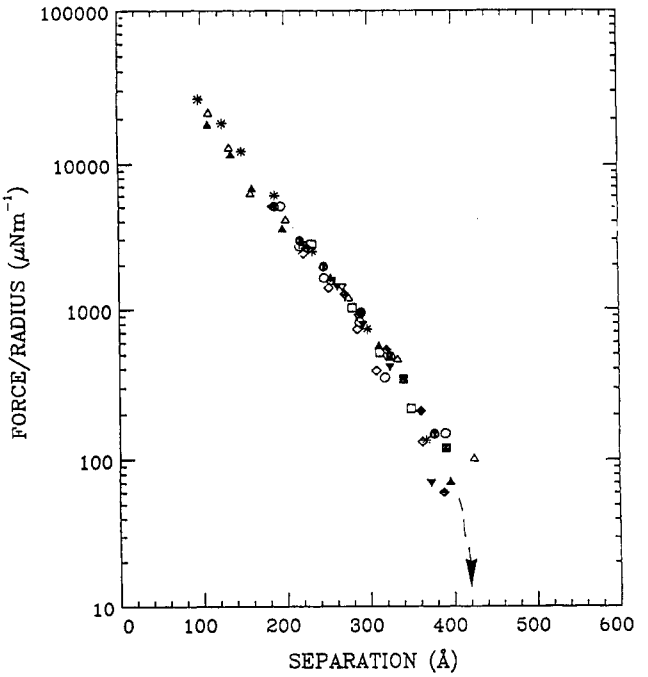

Figure 4. Force–distance profiles between curved mica sheets following incubation to saturation in a solution (ca. 10^{-4} w/w) of PS–X(26K) in toluene. Different rates of compression and decompression were used, and results are shown for two different experiments. The arrow indicates the separation below which the forces were below the detection limit of the apparatus (ca. 20 $\mu N \cdot m^{-1}$) in these experiments.

adsorbance was gradual and its increase could be observed over several h.[4,5] No attractive interactions—as might be due to bridging and as were observed in previous investigations (e.g., ref 5) at low surface coverage with adsorbed chains—were found even at the lowest experimentally accessible surface coverages.

Figures 4–9 show typical profiles following surface coverage to saturation for the PS–X and PS–PEO samples[36] of Tables I and II. The filled symbols show forces measured upon compression of the polymer layers, and the corresponding open symbols, the forces on subsequent decompression. Different rates of compression and decompression were used in all experiments, with the time taken to perform a single compression–decompression cycle being varied between 5 min and about 2 h, in a very similar manner to that described in ref 10 and 16 for adsorbed chains.

The qualitative features of all profiles are similar: a long-ranged repulsion, first observed at several radii of gyration of each polymer at a characteristic distance of onset of interaction and increasing monotonically at smaller separations. As shown in the profiles, there is no hysteretic behavior at rapid rates of compression and decompression, which is a characteristic feature of *adsorbed* chains in good solvents.[3,9,10,16] The profiles thus describe a quasi-equilibrium force–distance law; from the distance for onset of interaction, $2L_o$, which corresponds to

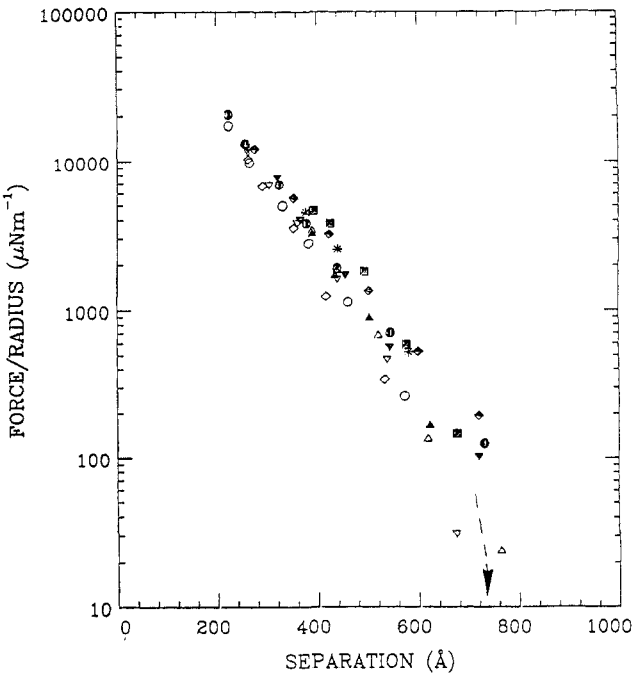

Figure 5. As in Figure 4 but for ca. a 10^{-4} w/w solution of PS-X(58K) in toluene.

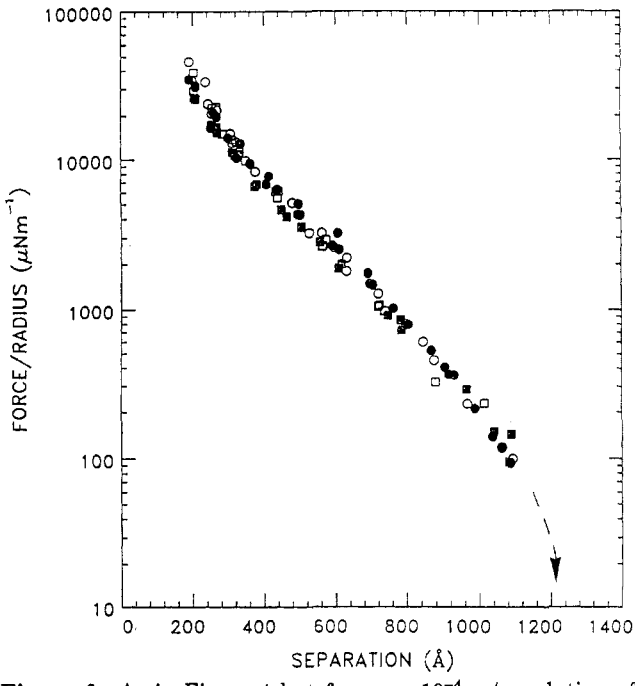

Figure 6. As in Figure 4 but for ca. a 10^{-4} w/w solution of PS-X(140K) in xylene (○, ●) and in toluene (□, ■).

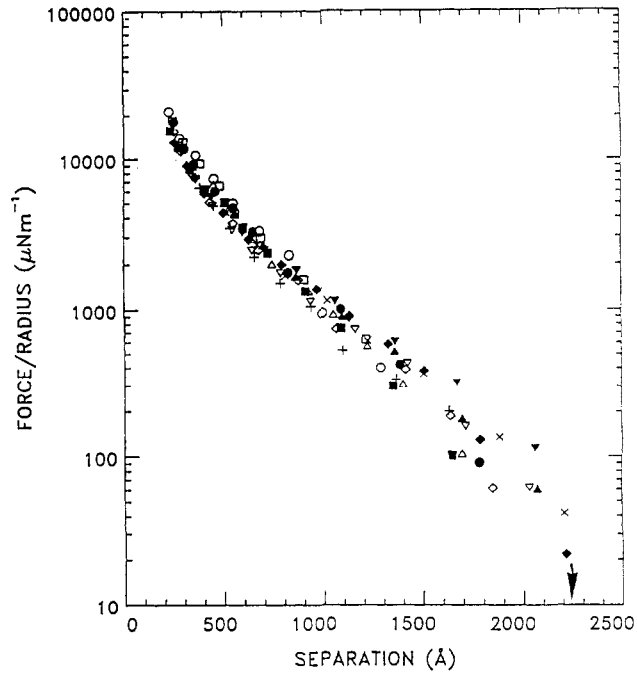

Figure 7. As in Figure 4 but for a ca. 10^{-4} w/w solution of PS-X(375K) in toluene.

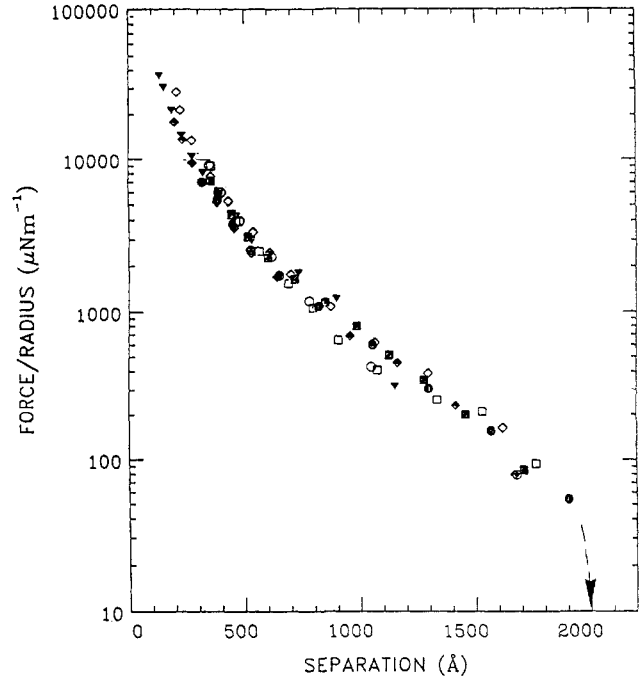

Figure 8. As in Figure 4 but for a ca. 10^{-4} w/w solution of PS-X(660K) in toluene.

the separation at which repulsion can just be detected, an effective layer thickness L_0 may be estimated. Mean values of $2L_0$, based on profiles as in Figures 4–9, are given in Table III as a function of the polymer molecular weight, while in Figure 10 L_0 is logarithmically plotted as a function of M for the PS–X chains. We note a good fit of the data (except for the longest PS–X chain) to the relation (solid line)

$$L_0 \propto M^{0.6}$$

This will be considered in a later section in the context of current theories.

Varying the concentration of the polymer solution by a factor of 10 during the incubation stage did not alter the observed layer thicknesses, an indication that saturation coverage had indeed been achieved. When the solution was replaced, following equilibration, by the pure solvent (resulting in a dilution by a factor of ca. 100), no change in the profiles was found, indicating an absence of any significant desorption as a result of this dilution. For a particular polymer identical profiles were obtained in both toluene and xylene. This is illustrated explicitly in Figure 6, where profiles for the PS-X(140K) sample in both xylene and toluene are shown and are the same within the experimental scatter.

The *shapes* of the interaction profiles were very similar for all molecular weights of both PS–X and PS–PEO. A summary of the profiles illustrating this point is shown in Figure 11, which contains data for one or two compressions–decompressions for each of the poly-

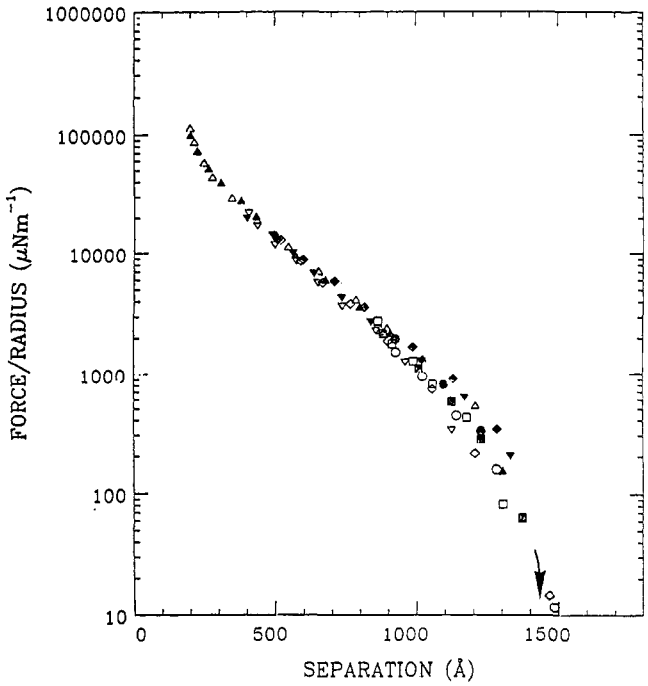

Figure 9. As in Figure 4 but for a ca. 10^{-4} w/w solution of PS–PEO(150K) in toluene.

Table III
Mean Surface Separations $2L_0$ at Onset of Detected Repulsion

sample	$2L_0$, Å
PS–X(26K)	440 ± 50
PS–X(58K)	800 ± 80
PS–X(140K)	1350 ± 100
PS–X(375K)	2400 ± 100
PS–X(660K)	2100 ± 100
PS–PEO(150K)	1450 ± 100
PS–PEO(184K)	1500 ± 100

mers used. The horizontal axis, which gives the separation of the mica surfaces, has been scaled empirically by the measured separation $2L_0$ at the onset of repulsion for each polymer (Table III), so as to give the thicknesses of the compressed layers as a fraction of their uncompressed values. The vertical axis, which describes the interaction forces between the surfaces, has also been shifted to enable the superposition on the master curve of Figure 11. We find that the magnitude of the forces for a given fractional compression varied with the molecular weight of the polystyrene chains; the superposition in Figure 11 is achieved by shifting the (logarithmic) vertical axes of the different force profiles, by amounts corresponding to factors that vary with the molecular weight. These shift factors are directly related to the extent of surface coverage.

For all molecular weights of both PS–X and PS–PEO the experiments were repeated at least twice and often several times, and the results obtained were reproducible to within the scatter in the data.

(d) Polymer on One Surface Only. Following the measurements of the equilibrium force–distance profile at saturation surface coverage, the polymer solution was replaced by pure solvent and the surfaces were separated. The upper mica sheet was then removed in a laminar-flow, clean-air cabinet and replaced by a clean mica sheet of the same thickness. In this way it was possible to measure the forces on compression of a single layer of terminally anchored, nonadsorbing polymer against the rigid wall provided by the bare mica sheet. This type of

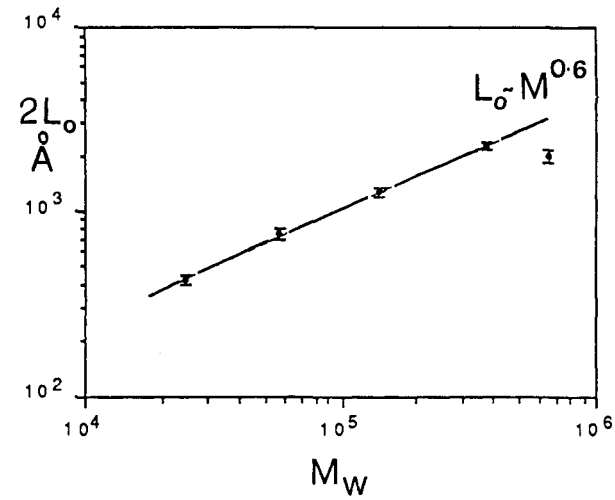

Figure 10. Double logarithmic plot of distance for onset of repulsion $2L_0$ between two mica surfaces, following incubation to saturation in solutions of PS–X, molecular weight M, in toluene.

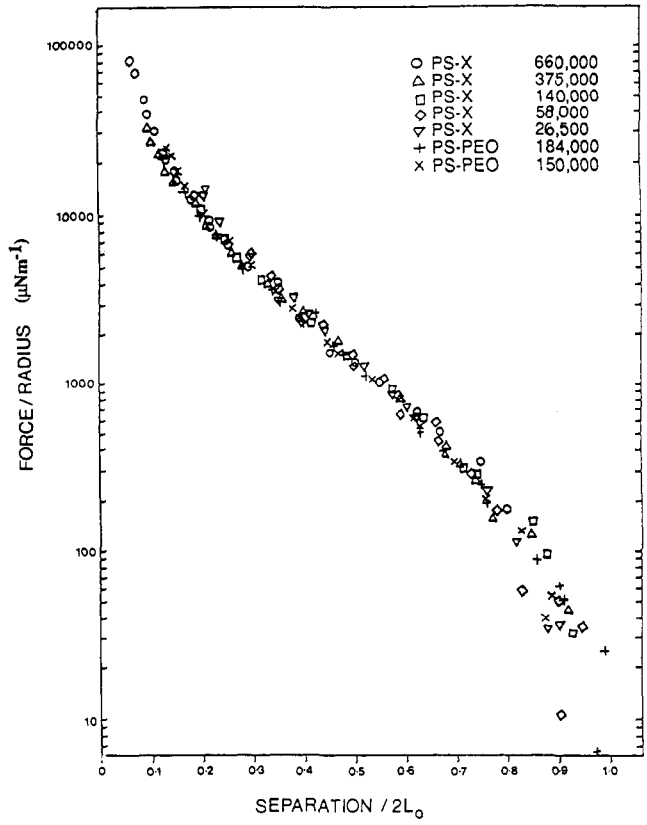

Figure 11. Master curve of force profiles incorporating data for all PS–X and PS–PEO samples. One or two compression–decompressions are shown for each polymer. The horizontal axis has been scaled by the separation $2L_0$ at which forces were first measured. Superposition of the profiles was achieved by multiplying the F/R values for each sample by an amount corresponding to the surface coverage.

measurement, where a mica sheet is replaced in the middle of an experiment, is particularly demanding and has a high failure rate, as revealed by the presence of long-ranged repulsion, which indicates surface contamination. Results from an experiment where no contamination was indicated, using PS–PEO(150K), are shown in Figure 12. The interaction observed was similar in form (being monotonically repulsive and nonhysteretic) but of shorter range than that found with the polymer attached to both surfaces. Most significant is the absence of any

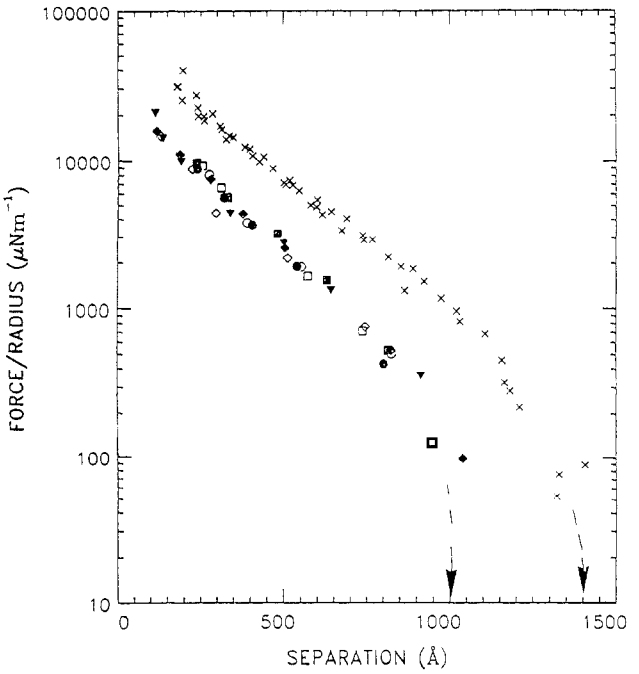

Figure 12. Forces between two curved mica sheets bearing end-anchored layers of PS–PEO(150K) (×) compared with forces following replacement of one of the coated surfaces with a clean mica sheet, as described in text (all other symbols).

attraction (on approach) or adhesion (upon separation) between the surfaces.

(e) Refractive Index Measurements. The optical technique in these experiments also permits the mean refractive index profile $n(D)$ of the medium between the surfaces (at separation D) to be measured, at the same time but independently of the force $F(D)$.[19,20] $n(D)$ in the pure solvent may be compared with $n(D)$ following surface coverage by the polymer, and an estimate of the surface coverage can then be made from the increase in the refractive index above that of the pure solvent at small separations. Such refractive index profiles are shown in Figure 13 for the case of pure toluene and following coverage to saturation by the PS–X(140K). From this data the surface coverage (for this polymer) was evaluated as 3 ± 0.5 mg/m^2 on each mica surface, corresponding to a mean distance s between the zwitterion–mica anchor points on the surface of ca. 85 Å.

IV. Discussion

The absence of any interaction over and above the pure solvent case when unfunctionalized PS is present in the system, contrasted with the strong, monotonic repulsion following addition of PS–X or PS–PEO, shows unambiguously that the latter are anchored to the surface by the –X group or short –PEO moieties only.[37] The resulting force profiles show a number of qualitative differences to the adsorbed polymer case: first, the *range* of the interaction is considerably larger, with repulsion being first measured at separations corresponding to some 12–14 R_g (see Tables I and III) over the range of molecular weights studied. In the case of adsorbed polymers, on the other hand, repulsions (following adsorbance to equilibrium) were first measured at surface separations of some 6–8 R_g over a comparable molecular weight range, for similar surface coverage by the polymers.[10,16,23] The thickness of the end-anchored layers is thus roughly twice that of the adsorbed layers for the same amount of polymer of the same size on the surface. Second, the absence of any bridging attraction, even following the shortest accessible incubation times, is in contrast with the behavior of adsorbed polymers in good solvents, which show marked attraction at low incubation times, i.e., low adsorbances.[4,5] The monotonic repulsion between the plates when one surface only is covered with grafted chains (Figure 12) is an even more striking illustration of the absence of bridging: similar measurements in the elegant study of Granick et al. with *adsorbed* chains[24] (polystyrene on mica in cyclohexane), where only one surface was covered with polymer, show a massive adhesive force ($\sim 3 \times 10^4$ μN·m) between the surfaces once they are brought into contact. The complete absence of any attraction or adhesion in our experiments confirms the nonadsorbing nature of the terminally anchored tails, which eliminates the possibility of bridging; it also demonstrates directly that such end-grafted, nonadsorbing species can be useful as stabilizers in conditions where adsorbed polymers would lead to flocculation.[1,2]

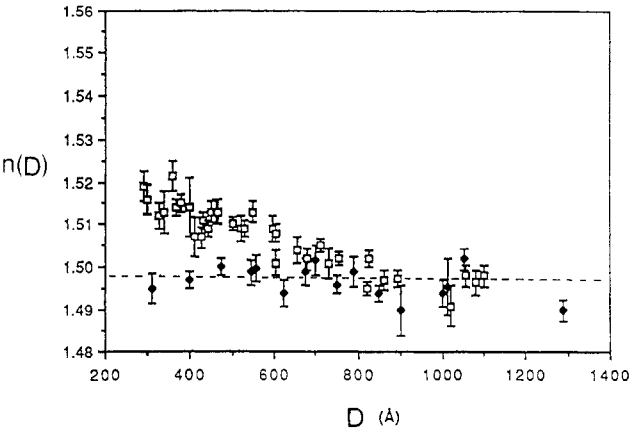

Figure 13. Refractive index $n(D)$ as function of separation D between curved mica sheets in pure toluene (◆) and following addition of PS–X(140K) to concentration ca. 10^{-4} w/w and coverage to saturation (□).

The use of a short length of the adsorbing polymer PEO rather than the zwitterionic group X as the anchor did not affect the interaction profiles, except possibly through the surface coverage, the shape of the profiles being identical within experimental error as illustrated in Figure 11. Thus the behavior of block copolymers containing one fairly short adsorbing block may be analyzed in terms of terminally anchored tails. It is noted from our results that only a small number monomers of the adsorbing species, on order of 100, were necessary in order to anchor the copolymers onto the surface in an apparently irreversible manner.[35]

Another noticeable feature of the interaction profiles is the absence of any *relaxation effects* following strong compression of the surfaces—at all accessible rates of approach and separation in our experiments—which can also be attributed to the nonadsorbing nature of the end-anchored PS tails (Figures 4–9). This is in strong contrast to the hysteresis or relaxation behavior observed at short times following compression of *adsorbed* layers in good solvents. Relaxation effects in the latter case were observed both in aqueous[10] and in organic solvents,[16] and at all molecular weights studied, to the extent that they became a "signature" of adsorbed layers;[9] the long times (on order of many minutes or even longer for long chains) taken for adsorbed layers—once they were strongly compressed—to recover their equilibrium configuration, were attributed[10] to the sluggish rate of *desorption* of monomers that had been forced onto the surfaces by the compression. Clearly for nonadsorbing chains such a com-

pressive adsorption would not occur.

The good reproducibility of our data and the absence of any time-dependent effects, taken together with the well-characterized nature of the surface structure of the chains—i.e., that they are anchored onto each mica sheet pointwise at one end only, with the polymer dangling into solution—invites a critical comparison with current molecular theories of end-anchored, nonadsorbing chains. These fall into two categories: scaling and mean field. In the former, due initially to Alexander,[25] chains of degree of polymerization N, grafted at one end to a surface with a mean spacing s between grafting points, extend out from the surface into the good solvent to form a layer of thickness L. For high surface densities, such that $s \ll R_F$ (the Flory radius), the grafted layer is in the semidilute regime and is assumed to have an essentially uniform concentration density away from the surface. Each chain is then taken to consist of connected semidilute "blobs"[32] with the osmotic repulsion between blobs tending to stretch the chains; this tendency is opposed by the increase in the *elastic* free energy of the chains when overstretched. By minimizing the overall free energy with respect to the layer thickness, Alexander found[25] that at equilibrium each grafted polymer could be considered as a chain of blobs each of size s, stretching away from the surface, with the equilibrium layer thickness $L = L_0$ given by

$$L_0 = s(R_F/s)^{5/3} \tag{1}$$

i.e.

$$L_0 = Ns^{-2/3}a^{5/3} \tag{2}$$

putting $R_F = N^{3/5}a$, where a is a monomer size. We note especially the linear dependence of L_0 on the chain size N and also that—as in all scaling models—a numerical prefactor of order unity is missing in eq 1 and 2.

de Gennes extended[26] these ideas to the case of the interaction force per unit area $f(D)$ between two parallel plates a distance D apart bearing such grafted layers, obtaining

$$f(D) = k_BT/s^3[(2L_0/D)^{9/4} - (D/2L_0)^{3/4}] \qquad D < 2L_0 \tag{3}$$

again to within an undetermined prefactor of order unity. Here k_B and T are Boltzmann's constant and the temperature, respectively. In eq 3 the first term in square brackets derives from the increasing osmotic repulsion as the surfaces are compressed to smaller D (with correspondingly higher mean monomer concentrations in the gap between the surfaces); the second term in square brackets is due to the reduction in free energy as the overstretched chains in the grafted layers are compressed closer to their equilibrium configuration. This picture assumes that little mutual interpretation takes place between layers as they are compressed together. As soon as D becomes appreciably lower than $2L_0$, the osmotic repulsion term dominates.

There are a number of mean-field calculations of the structure of adsorbed diblock copolymers and end-grafted chains.[27-30] The closest to our model experimental configuration is that by Milner, Witten, and Cates,[30] who treated end-grafted polymer chains using a self-consistent mean-field approach. An important difference between their model and that of Alexander is that they calculated a parabolic concentration profile for their grafted layers (in contrast to the uniform flat profile assumed by Alexander). In terms of the observables in our experiments, however, such as the layer thickness L_0 and the detailed force–distance profiles, their results are rather close to the Alexander–de Gennes predictions. For example, they derive[30]

$$L_0 = (12/\pi^2)^{1/3}w^{1/3}s^{-2/3}Na^{5/3} \tag{4}$$

for the equilibrium layer thickness, which differs from eq 2 only by the numerical prefactor $(12w/\pi^2)^{1/3}$, where w is an excluded-volume parameter. Again, the detailed force calculations in the mean-field model, though evaluated by rather different methods to the scaling model, yield interaction–distance profiles that are quite similar. We shall therefore find it convenient in the subsequent discussion to relate mostly to the scaling results.

The system for which we have the fullest characterization is PS–X(140K), for which s (≅85 Å) is explicitly determined from our refractive index profile (Figure 13). We note that the validity regime of the theoretical models[25,30] is obeyed in this system: thus $s \cong (1/4)R_F$ (see Table I), while the mean monomer concentration in the (uncompressed) end-adsorbed layers, corresponding to the adsorbance 3 ± 0.5 mg·m^{-2}, is around 4%, well within the semidilute regime. We may thus assume that our experimental conditions correspond closely to the model assumptions. Putting in values of s and R_F (Table I) into eq 1 (with an implicit prefactor of unity), we find

$$L_0 = 740 \pm 50 \text{ Å} \qquad \text{scaling prediction} \tag{5}$$

compared with the experimental L_0, taken as half the distance for onset of interaction (Table III), given by

$$L_0 = 650 \pm 50 \text{ Å} \qquad \text{experimental} \tag{5a}$$

The mean-field result, evaluated for this specific case by Milner,[31] is also close to the experimental L_0. We recall that the scaling prediction (eq 5) is derived within an undetermined factor of order unity (the scatter in the predicted value (eq 5) is due to uncertainty in s and R_F).

Knowing s and L_0, we may also plot the full force profile, from eq 3. Our experimental data is plotted in terms of $(F(D)/R)$, which in the Derjaguin approximation (valid for our geometry) is related to the surface energy $E(D)$ per unit area between two flat parallel plates a distance D apart, obeying the same force–distance law as[19,20]

$$F(D)/R = 2\pi E(D) \tag{6}$$

$E(D)$ is related to the force per unit area, $f(D)$ in eq 3, as

$$E(D) = \int_{2L_0}^{D} f(D')\,dD' \tag{7}$$

so that from eq 6 and 7 our results may be directly compared with the scaling prediction of eq 3. This is shown in Figure 14 for PS–X(140K), for s = 85 Å and L_0 = 650 Å, as determined in our measurements. The fit, over nearly 4 orders of magnitude in F/R, is close. The prefactor necessary in eq 3 to give the fit shown is 1.5; i.e., the scaling expression is *quantitatively* correct to within this factor. Detailed calculations by Milner,[31] based on the mean-field approach, also give a close fit of the predicted force profile to that observed with PS–X(140K) (inset to Figure 14). The general shape of the predicted profile, and its variation with D, fits closely also to the other PS–X and PS–PEO profiles, as indicated by the data (which include PS–X(140K)) in Figure 11.

Both the scaling[25] (eq 2) and the mean-field approach[30] (eq 4) predict a grafted layer thickness L_0 varying linearly with the molecular weight M (or degree of polymerization N) for the high surface density regime ($s \ll R_F$), for a given interanchor spacing s. The actual vari-

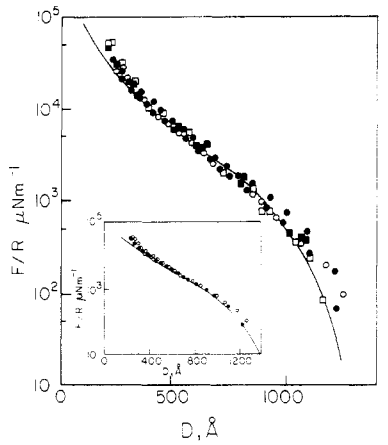

Figure 14. Comparison of force profile F/R vs D for PS–X(140K) with the Alexander–de Gennes model (see eq 3, 6, and 7) using the experimentally determined values L_0 = 650 Å and s = 85 Å; the fit shown requires a prefactor of 1.5 in eq 3. The inset (taken from ref 31) shows the data and calculated profile based on the Millner–Witten–Cates model, using a surface coverage of 3.5 mg·m^{-2} of the polymer on each surface (compared with the experimentally estimated coverage 3 ± 0.5 mg·m^{-2}) but no other adjustable parameters.

ation, shown in Figure 10 (also Table II), is different:

$$L_0 \propto M^{0.6} \text{ (or } N^{0.6}) \tag{8}$$

We may go some way toward resolving the discrepancy between theory (eq 2 or 4) and experiment (eq 8) by bearing in mind that in our experiments with PS–X it is not s that is fixed but rather the *interaction energy* —between the zwitterion –X and the mica surface—that is constant between one PS–X sample and another of a different length. We may assume that, at equilibrium, the surface coverage by each PS–X is such that the overall repulsive energy per molecule, due to being attached to the surface (and resulting from the osmotic interaction with its neighbors), is *just balanced* by the sticking energy, $\alpha k_B T$, due to the zwitterion–mica interaction, where α is a constant; this allows us to deduce how s, and thus L_0, should vary with N. In the Alexander picture[25] each chain consists of (N/g) blobs stretching away from the surface, where g is the number of monomers in a blob, and the blob size equals the mean interanchor spacing s. Thus

$$s = g^{3/5}a \tag{9}$$

Since the excess repulsive energy per blob in a good solvent is ca. $k_B T$, we expect the overall excess repulsive energy per chain to be on the order of $(N/g)k_B T$ and to be just balanced by the sticking energy, $\alpha k_B T$; i.e., the number of blobs per chain (N/g) is constant (and on the order of α), so that $g \propto N$ and (from eq 9)

$$s \propto N^{3/5} \tag{10}$$

Thus from eq 2 and 10

$$L \propto N^{3/5} \tag{11}$$

which is indeed the observed variation of Figure 10.

We may also estimate s as a function of N by considering the interaction profile for each PS–X sample. We do this by observing that at high compressions the interaction is dominated by the osmotic segment–segment repulsion within the intersurface gap; this can be used to estimate the mean segment density, and, hence, the overall absorbance, within an unknown constant. Since we know s explicitly ($s \cong 85$ Å) for PS–X(140K), the unknown

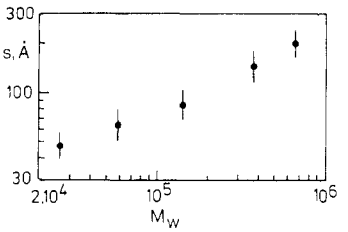

Figure 15. Double logarithmic plot of mean interanchor spacing s of PS–X(M) on the mica surfaces, as a function of M, estimated from the high-compression portion of the force profiles as described in the text (eq 16).

constant may be evaluated and s explicitly determined for all the PS–X samples. We proceed as follows: we choose a given (high-compression) value of the interaction energy, $E(D')$, where D' is the corresponding surface separation. At sufficiently high compressions we may assume the monomer concentration $\phi(D)$ in a gap D is uniform, being given by

$$\phi(D) = 2\Gamma\nu/D \tag{12}$$

where Γ is the polymer surface excess per unit area and ν is the specific volume, and the pressure between the plates equals the osmotic pressure $\Pi(\phi(D))$. We may also use the Flory–Huggins mean-field approximation,[38] $\Pi(\phi) \cong$ constant $\times \phi^2$, and approximate the interaction energy $E(D')$ as[39]

$$E(D') = \int_{2L_0}^{D'} \Pi(\phi(D))\, dD \tag{13}$$

$$\cong \text{constant} \times (\Gamma^2/D') \tag{14}$$

Now the interanchor spacing, s, is related to Γ, for a given M, as

$$s \propto (\Gamma/M)^{-1/2} \tag{15}$$

Hence, substituting for Γ from eq 14, we have

$$E(D') = \text{constant} \times (M^2/D's^4)$$

so that for a *given* $E(D')$

$$s = \text{constant} \times (M^{1/2}/D'^{1/4}) \tag{16}$$

The value of the constant in eq 16 is determined by setting s = 85 Å for $M = 140 \times 10^3$. We choose, for each PS–X sample, the D' value corresponding to the high compression, $F(D')/R = 10^4$ μN·m^{-1} ($=2\pi E(D')$, from eq 6) taken from Figures 4–8. The variation of s with M is shown in Figure 15, where the uncertainty in s is due to the scatter in the force–distance profiles and hence in D'. The overall trend is clear: s increases with increasing molecular weight of the PS–X chains, as qualitatively expected from our discussion above, though the variation is somewhat weaker than the simple scaling result of eq 10.

For a variable surface density of end-adsorbed chains, then, both the scaling[25] and the mean-field[30] relations (eq 2 and 4, respectively) predict that it is not the layer thickness L_0 that should vary with N but rather the product $L_0 s^{2/3}$. In Figure 16 this product is plotted against M for the PS–X samples. The data are well described by a power law relation (solid line, Figure 16)

$$L_0 s^{2/3} = \text{constant} \times N^{\beta} \tag{17}$$

where $\beta = 0.90 \pm 0.1$, which compares closely with the value $\beta = 1$ expected from both mean-field and scaling approaches.

The deviation from the relation of eq 17 of the data for the highest M sample, the PS–X(660K), may be due

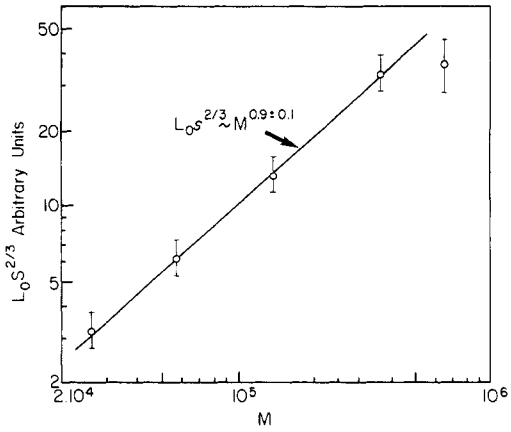

Figure 16. Double logarithmic plot of the variation of $L_0s^{2/3}$ (arbitrary units) with M for PS-X(M) (see eq 17).

to the rather sparse density of these longest end-anchored chains on the surface (see Figure 15): in this case an anomalously large interpenetration of the opposing layers may be required—for our apparatus to detect repulsion—relative to the lower M PS-X samples, leading to the rather low effective L_0 observed (Figure 10) for this sample. The effect of such interpenetration has been considered in detail in ref 23, and, to a lesser extent, it may also be responsible for the experimental value of β being slightly lower than the theoretical prediction $\beta = 1$. We mention in passing that, in terms of the scaling model, the number of "blobs" in each end-adsorbed chain is on the order of L_0/s, which is ca. 6–8 over the range of PS-X samples studied (Table III and Figure 15). Our earlier assumption (following eq 9) that, at equilibrium, the sticking energy αk_BT corresponds to about α blobs per chain then sets the zwitterion–mica interaction at a value of order 6–8 k_BT, a reasonable magnitude for this type of interaction and one also comparable with that deduced on the basis of the PS-X(140K) data in the mean-field calculations.[31]

It finally remains to consider the time-dependent aspects of the adsorption and desorption process of the end-anchored chains. As noted in Results, the times associated with surface coverage to equilibrium of the anchoring zwitterion end group (or PEO moiety) onto the mica were much shorter than those for corresponding chains undergoing adsorption (e.g., PS in cyclopentane[4] or PEO in water[5]). Qualitatively, one may imagine that, in the case of adsorbing chains, the adsorption of the first polymer molecules reaching the bare surface results in a nonequilibrium (probably quite flat) configuration; the arrival at the surface of subsequent chains leads to rearrangement, including partial desorption of the first chains, and the eventual equilibrium configuration, which involves many overlapping adsorbed chains on the surface. More detailed considerations of this picture have appeared.[33] For the end-anchored chains, however, once the end moiety of a chain has adhered to the mica (with a sticking energy $\gg k_BT$), no further desorption is necessary to accommodate additional chains on the surface (as in the rearrangement of *adsorbed* chains) and the rate of surface coverage is controlled by the arrival rate of anchoring end groups at the surface.

The last point concerns the absence of *desorption* over the times of our experiments, even at the highest compressions in our investigations, which correspond to compressive energies of ca. $100k_BT$ per anchored chain. This we also attribute to kinetic factors: while these large compressive forces are certainly sufficient to overcome the sticking energies, which are on the order of $10k_BT$ per chain, the compressed polymer in the gap between the surfaces is in a highly entangled state, with a correspondingly low (reptative) diffusion rate.[33] Moreover the diffusion of chains with "sticky" ends close to a surface is further suppressed as the sticking energy provides an effective potential gradient opposing the diffusion of the ends away from the surface. We interpret the absence of desorption in our compression experiments as due to the slowness of these diffusive processes.

To summarize, we have found that nonadsorbing polymer chains (PS-X or PS-PEO) terminally attached at a solid–liquid interface take up extended configurations, with measured layer thicknesses L_0 being roughly twice that found for adsorbing chains of the same length and at comparable surface coverages. The rate of surface coverage from the polymer solution is rapid compared with adsorbed chains, probably because once the ends attach to the surface little further rearrangement is necessary. The attachment, which is achieved either by a single zwitterionic group (X) or by a very short length of adsorbing polymer moiety (PEO), is irreversible in the time scale of our experiments, even when two polymer-bearing surfaces are strongly compressed against each other: this is likely to be due to the very slow diffusion of polymers in the compressed surface layers. For the PS-X, L_0 was found to vary as the 0.6 power of the PS molecular weight, while the interanchor spacing s at equilibrium surface coverage increased with M. No evidence of attraction between the surfaces at low surface coverage, an effect characteristic of adsorbing chains, was detected. The forces between the surfaces were found to be monotonically repulsive and not to vary with the rates of compression–decompression used, again in contrast to adsorbing chains. Both the latter effects are expected for nonadsorbing monomers.

Detailed comparison of our model experiments with scaling and mean-field models suggests that both can account quantitatively for the main features of our results. These include the absolute magnitudes of L_0, the shapes of the force–distance profiles, and the quantity $L_0s^{2/3}$, which we find to vary almost linearly with M, as predicted both by the scaling and by the mean-field approach.

Acknowledgment. We are grateful to Tim Nicholson and Rachel Yerushalmi-Rozen for their help. J.K. thanks Matthew Tirrell for useful discussions and Tom Witten for illuminating comments. H.J.T. thanks the SERC (U.K.) and Unilever (plc) for a CASE award, and C.T. thanks Sir Geoffrey Allen for encouragement and support. This work was supported by the Israeli Academy (Basic Research Division) and by the Minerva Foundation.

References and Notes

(1) Vincent, B. *Adv. Colloid Interface Sci.* **1974**, *4*, 193.
(2) Napper, D. H. *Polymeric Stabilisation of Colloidal Dispersions*; Academic Press: London, 1983.
(3) Klein, J. In *Molecular Conformation and Dynamics of Macromolecules in Condensed Systems*; Nagasawa, M., Ed.; Elsevier: Amsterdam, Holland, 1988; pp 333–352.
(4) Almog, Y.; Klein, J. *J. Colloid Interface Sci.* **1985**, *106*, 33.
(5) Klein, J.; Luckham, P. F. *Nature* **1984**, *308*, 836.
(6) Fleer, G. J.; Lyklema, J. *J. Colloid Interface Sci.* **1974**, *46*, 1.
(7) Dolan, K.; Edwards, S. F. *Proc. R. Soc.* **1974**, *337A*, 509.
(8) Homola, A. N.; Robertson, A. A. *J. Colloid Interface Sci.* **1976**, *54*, 286.
(9) Luckham, P. F.; Klein, J. *J. Colloid Interface Sci.* **1987**, *117*, 149.
(10) Luckham, P. F.; Klein, J. *Macromolecules* **1985**, *18*, 721.
(11) Hadziioannou, G.; Granick, S.; Patel, S.; Tirrell, M. *J. Am. Chem. Soc.* **1986**, *108*, 2869.

(12) Ansarifar, A.; Luckham, P. F. *Polymer* **1988**, *29*, 329.
(13) de Gennes, P. G. *Adv. Colloid Interface Sci.* **1987**, *27*, 189.
(14) Taunton, H. J.; Toprakcioglu, C.; Klein, J. *Macromolecules* **1988**, *21*, 3333.
(15) Klein, J.; Luckham, P. F. *Nature* **1982**, *300*, 429; *Macromolecules* **1984**, *17*, 1048.
(16) Brief accounts of some preliminary data have appeared earlier. See: Taunton, H. J.; Toprakcioglu, C.; Fetters, L. J.; Klein, J. *Nature* **1988**, *332*, 712 and ref 14.
(17) Davidson, N. S.; Fetters, L. J.; Funk, W. G.; Graessley, W. W.; Hadjichristidis, N. *Macromolecules* **1988**, *21*, 112.
(18) Tabor, D.; Winterton, R. H. S. *Proc. R. Soc.* **1969**, *A312*, 435. Israelachvili, J. N.; Tabor, D. *Proc. R. Soc.* **1972**, *A331*, 19.
(19) Israelachvili, J. N.; Adams, G. *J. Chem. Soc., Faraday Trans. 1* **1978**, *79*, 975.
(20) Klein, J. *J. Chem. Soc., Faraday Trans. 1* **1983**, *79*, 99.
(21) Terashima, H.; Klein, J.; Luckham, P. F. In *Adsorption from Solution*; Ottewill, R., Rochester, C., Eds.; Academic: London, 1983; p 299.
(22) Christenson, H. Ph.D. Thesis, Australian National University, Canberra, 1983.
(23) Klein, J.; Luckham, P. F. *Macromolecules* **1986**, *19*, 2007.
(24) Granick, S.; Patel, S.; Tirrell, M. *J. Chem. Phys.* **1986**, *85*, 5370.
(25) Alexander, S. *J. Phys. (Paris)* **1977**, *38*, 983.
(26) de Gennes, P. G. *C. R. Hebd. Seances Sci.* **1985**, *300*, 839.
(27) Dolan, A. K.; Edwards, S. F. *Proc. R. Soc.* **1975**, *A343*, 427.
(28) Marques, C.; Joanny, J. F.; Leibler, L. *Macromolecules* **1988**, *21*, 1051.
(29) Munch, M. R.; Gast, A. P. *Macromolecules* **1988**, *21*, 1366.
(30) Milner, S.; Witten, T.; Cates, M. *Macromolecules* **1988**, *21*, 2610. See also: Muthukumar, M.; Ho, J.-S. *Macromolecules* **1989**, *22*, 965.
(31) Milner, S. *Europhys. Lett.* **1988**, *7*, 695.
(32) de Gennes, P. G. *Scaling Concepts in Polymer Physics*; Cornell University Press: Ithaca, 1979.
(33) See for example: de Gennes, P. G. Reference 3; p 315, and references therein.
(34) The data of ref 11 and 12 and their relation to the force profiles using PS-PEO diblock copolymers in the present study, including the interesting possibility of micellization of the PS-PVP diblock (see: Tang, W. T.; Hadziioannou, G.; Cotts, P. M.; Frank, C. W.; Smith, B. A. *Macromolecules*, in press) has been considered in more detail in ref 14.
(35) PEO is known to adsorb strongly onto mica from toluene, from earlier investigations:[10] we note, however, that a minimal length of the PEO moiety was found to be necessary in order to ensure anchoring of the PS tail as described in this paper. Thus, for a different PS-PEO sample where the PEO content was less than 0.3%, the force measurements (not shown) indicated a very weak adsorbance and a force-distance law qualitatively different to that of Figures 3-9.
(36) The force profile for PS-PEO(184K) is given in ref 14.
(37) We observe no evidence of PS-X micellizing in the toluene or xylene; more direct evidence for absence of any micellization in a very similar system, polyisoprene-X in toluene, is presented in ref 17. Moreover, there is no evidence for PS-PEO in micellizing in toluene, a good solvent for both blocks (also: Gast, A. P., private communication).
(38) At the monomer concentrations, in the gap between the surfaces, associated with the high compressions $E(D')$, which are around $\phi \cong 0.1$, the approximation $\Pi(\phi) \propto \phi^2$ is good to about 1% (within the Flory-Huggins model). Use of the scaling expression $\Pi \propto \phi^{9/4}$ would not make a great difference in view of the spread in D' due to the scatter in the magnitude of the forces.
(39) We ignore the (weak) elastic contribution to $f(D)$ appearing in eq 3 and also neglect $\Gamma^2/(2L_o)$ relative to Γ^2/D', both of which are good approximations at $D' \ll 2L_o$.
(40) R_o for PS in toluene is evaluated from[41] $R_o = 0.69M_w^{0.5}$ (Å) while R_F for PS in toluene is evaluated from[42] $R_F = 0.32M_w^{0.585}$ (Å) where M is the PS molecular weight, from ref 41 and 42.
(41) Roovers, J. E.; Bywater, S. *Macromolecules* **1972**, *5*, 385.
(42) Roovers, J. E.; Toporowski, P. M. *J. Polym. Sci., Polym. Phys. Ed.* **1980**, *18*, 1907.

Registry No. PS, 9003-53-6; (EO)(S) (block copolymer), 107311-90-0; toluene, 108-88-3; xylene, 1330-20-7.

Validity of Some Approximations Used To Model Intramolecular Reaction in Irreversible Polymerization

Claudia Sarmoria and Enrique M. Vallés*

Planta Piloto de Ingeniería Química, UNS-CONICET, CC 717, 8000 Bahía Blanca, Argentina

Douglas R. Miller

George Mason University, ORAS, SITE, Fairfax, Virginia 22030.
Received December 1, 1988; Revised Manuscript Received July 15, 1989

ABSTRACT: We identify the main approximations underlying several methods that have been used to model stepwise, irreversible copolymerizations with intramolecular reaction allowed, and we study their ranges of validity. In order to do this, all approximations are applied to the linear $A_2 + B_2$ system, for which comparison against an exact solution is possible. We also combine approximations found in different models to give "hybrid" models. We have found that for this linear system some approximations never give good results, others may be used when ring formation is low, and the better ones may be applied with low to moderate levels of intramolecular reaction. None of them is satisfactory when ring formation is very high.

Introduction

Modeling of intramolecular reaction in stepwise, irreversible polymerization is an old problem that has not been completely solved for most systems. When the monomers have only two reactive sites (linear system), the problem can in principle be solved to any desired degree of accuracy using either a purely kinetic[1,2] or a kinetic recursive[3] model. Network-forming systems are much more complicated, and no exact solution is available for them. Modeling of such systems has been attempted using approximate treatments such as spanning tree,[4,5] rate theory,[6-8] or kinetic recursive[3] methods. Each of these methods is based on one or more approximations with varying degrees of accuracy; the models will be as reliable as the approximations on which they are based.

In this paper we study the range of validity of some of these approximations as applied to the linear system, where

0024-9297/90/2223-0580$02.50/0